



Surfactant control of gas transfer velocity along an offshore coastal transect: results from a laboratory gas exchange tank

R. Pereira¹, K. Schneider-Zapp¹, R. C. Upstill-Goddard¹

¹School of Marine Science and Technology, Newcastle University, Newcastle upon Tyne, NE1 7RU, UK

5 Correspondence to: R. Pereira (Ryan.Pereira@ncl.ac.uk)

Abstract.

We measured total surfactant activity (SA; Triton T-X-100 equivalent) and CDOM absorbance (cm^{-1}) in the surface microlayer (SML) and subsurface water (SSW) seasonally (2012-2013) along a 20 km coastal transect (North East UK), and evaluated corresponding values of the gas transfer velocity (k_w ; cm hr^{-1}) using a custom-designed air-sea gas exchange tank. Spatial SA variability exceeded its temporal variability. Overall, SA varied five-fold between all samples (0.08 - 0.38 mg L^{-1} T-X-100), being highest in the SML during summer. SML SA enrichment factors relative to SSW were $\sim 1.0 - 1.9$, except for two values (0.75; 0.89; February 2013). CDOM absorbance (250 - 450 nm), the CDOM spectral slope ratio ($S_R = S_{275-295} / S_{350-400}$) and the 250:365 nm CDOM absorbance ratio ($E_2 : E_3$) demonstrate the potential for terrestrially-derived CDOM to be biogeochemically processed in North Sea coastal waters. The range in corresponding k_{660} (k_w for CO_2 ; freshwater; 20 °C) was 6.8 - 22.0 cm hr^{-1} . The film factor R_{660} (the ratio of the scaled transfer velocity k_{660} to the one of clean water) strongly correlates with SA ($r \geq 0.70$, $p \leq 0.002$, each $n = 16$) with high SML SA correlated to k_{660} suppression $\sim 14 - 51\%$ relative to clean laboratory water, highlighting strong spatio-temporal gradients in gas exchange due to varying surfactant in these coastal waters. Such variability should be taken account of when evaluating marine trace gas sources and sinks.

Introduction

Climate active gases such as carbon dioxide (CO_2), nitrous oxide (N_2O) and methane (CH_4) have important marine sources and sinks that are predicted to change in a future climate (Bakker et al., 2014). For CO_2 , uncertainty over the environmental controls of its water-side gas transfer velocity (k_w) is the greatest obstacle to accurately evaluating the global net air-sea flux (Takahashi et al., 2009). Environmental control of k_w is exerted through the modification of turbulent diffusion at the air-sea interface (Upstill-Goddard, 2006). Wind speed is the most fundamental control but its use for predicting k_w is compromised by high data scatter that is unrelated to methodological issues (Asher, 2009). The result is several parameterizations (e.g. Nightingale et al., 2000; Wanninkhof, 1992; Wanninkhof et al., 1997; Wanninkhof and McGillis, 1999) with differences that imply variable influences from other factors such as atmospheric stability, sea state, breaking waves, white caps, bubble transport, rain and the presence of surfactants and organics (Upstill-Goddard, 2006).

Soluble and insoluble surfactants, both natural and anthropogenic (Gašparović et al., 1998; Petrović et al., 2002; Žutić et al., 1981), decrease turbulent energy transfer at the air-sea interface and act as a monolayer physical barrier (McKenna and McGillis, 2004). While k_w suppression by surfactant $\sim 5-55\%$ has been observed in the



laboratory (Bock et al., 1999; Goldman et al., 1988) and at sea (Brockmann et al., 1982; Salter et al., 2011), this has mostly involved artificial compounds. The role of natural surfactants has remained inadequately quantified due to procedural difficulties (Salter et al., 2011). Schmidt and Schneider (2011) have estimated the change of k_w in small seawater samples from O_2 transfer versus the reduction of surface tension with respect to surfactant-free water and suggested a seasonal variability associated with surfactant concentration. However, a critical knowledge gap still exists and we estimated the temporal variability in k_w along an offshore gradient in natural surfactant, using a laboratory gas exchange tank custom built for this purpose.

45 **Materials and Methods**

Sampling was at five, 5 km spaced stations along the Dove Time Series (DTS; Fig. 1) transect off the North East UK coast, using RV *Princess Royal*. Sampling locations are listed in Table 1. At each station the sea surface microlayer (SML) and sub-surface water (SSW) were each sampled in triplicate. Following a well-established protocol (Cunliffe et al., 2014), the SML was collected using a Garret Screen (Garrett, 1965; mesh 16, wire diameter 0.36 mm, opening 1.25 mm), transferred to 50 mL high density polyethylene (HDPE) bottles and stored in an on-board refrigerator at 4 °C (Cunliffe et al., 2013; Schneider-Zapp et al., 2013). SSW (~100 litres) was sampled from a non-toxic supply pump located ~1 m below the water surface and collected in 5 x 20 L HDPE carboys that were pre-cleaned with 20% HCl to remove leachable organics. On return to the laboratory, typically within 6 hours of sampling, all samples were stored in a 4 °C dark cold room (Schneider-Zapp et al., 2013).

55 Surfactant activity (SA) in the SML and SSW was measured in triplicate by phase-sensitive AC voltammetry (797 VA Computrace: Metrohm, Switzerland) using a hanging mercury drop (Ćosović and Vojvodić, 1982) with sample salinities pre-adjusted to 35.0 via the addition of surfactant-free 3 mol L⁻¹ NaCl solution. Calibration was against the non-ionic soluble surfactant Triton T-X-100. All equipment was acid-washed (10% HCl) and analytical grade water-rinsed (18.2 Ohm Milli-Q, Millipore System Inc., USA) prior to use.

CDOM absorbance (wavelength range 800 - 250 nm) was determined in 1 nm steps by UV-Vis spectrophotometry (Varian Cary 100 Bio; Varian Inc, USA) using 10 cm path length quartz cuvettes, rinsed three times with ultra-pure water (Milli-Q: Millipore System Inc., USA). Spectra were blank corrected using Milli-Q water and for machine drift using the mean absorption from 700 nm to 800 nm. Measurements were made in triplicate and Naperian absorbance coefficients a (m⁻¹) were determined following Hu et al. (2002). For each measurement the mean value and standard error of the mean is reported. The 250:365 nm absorption ratio ($E_2 : E_3$) was used to track relative changes in low molecular weight (LMW) vs high molecular weight (HMW) dissolved organic matter (DOM); $E_2 : E_3$ decreases with increasing DOM molecular size due to increasing light absorption by HMW CDOM towards longer wavelengths (Peuravuori and Pihlaja, 1997). Spectral slope (S) was calculated using a nonlinear fit of an exponential function to the absorption spectrum over the ranges 275nm - 295nm and 350nm - 400nm, after Helms et al. (2008). The spectral slope ratio, S_R ($= S_{275-295} / S_{350-400}$), was used to broadly characterize CDOM in terms of molecular weight and source; DOM samples with low S_R are of high molecular weight and have a greater tendency to be allochthonous (Helms et al., 2008). Due to instrument maintenance no CDOM measurements are available for the 17/07/13 survey.

75



The SSW samples were used to estimate the variability in k_w using a fully automated, closed air–water gas exchange tank, the design, operation and routine rigorous cleaning of which are all described in detail in Schneider-Zapp et al. (2014). In brief, the system generates controllable and reproducible water-side turbulence with an electronically operated baffle. Although turbulence created in a laboratory tank inevitably differs from

80 turbulence *in situ*, which is primarily wind-driven, our overall aim was to derive a fundamental process understanding of the spatial and temporal controls of k_w variability. Therefore, our critical consideration was the maintenance of well-defined and reproducible conditions of turbulence that would facilitate this. Our experimental system meets this requirement while at the same time avoiding the practical complications of simulating wind-induced turbulence in a laboratory (Schneider-Zapp et al., 2014). Only when this process

85 understanding is established will more complex experiments involving wind-driven turbulence and relating the k_w estimates to those *in situ* be more appropriate.

Two coupled gas chromatographs (GC's) and an integral equilibrator, connected to the tank in a continuous gas-tight system, allow temporal changes in the partial pressures of SF₆, CH₄ and N₂O to be measured simultaneously

90 in the tank water and headspace at multiple turbulence settings, for each facilitating three independent estimates of k_{660} , i.e. the value of k_w for a Schmidt Number (Sc) = 660, where Sc is the ratio of kinematic viscosity to gas diffusivity and assuming a Schmidt Number exponent of 0.5 for a wavy surface (Upstill-Goddard, 2006). As the work presented here pre-dates the installation of an analytical capability for N₂O reported in Schneider-Zapp et al. (2014) our k_{660} estimates are based on CH₄ and SF₆ only.

To ensure that there are no losses of tracer gas, biogenic effects, or large amounts of analytical drift, the total mass was calculated from the measured partial pressures of CH₄ and SF₆ and the water and air volumes over the temporal evolution of the experiment (mass balance; Schneider-Zapp et al., 2014, Eq. 14). Experiments with a significant mass balance error (more than ±5 % drift throughout the entire experiment) were excluded. Most of our SF₆ measurements were affected, because they were outside the linear detection range of the electron capture

100 detector of the GC. As a result, we have not conducted any further analysis on the SF₆ dataset despite the values of k_{660} derived using SF₆ corresponding well with values derived from CH₄.

The uncertainty for each k_{660} measurement was derived via Gaussian error propagation (Schneider-Zapp et al., 2014; Tayler, 1996) and is typically smaller than ±0.8 cm hr⁻¹ (n = 48). We ascribe one result outside this range

105 (±3.9 cm hr⁻¹) to salt crystal formation that we observed in the water equilibration circuit. To clarify the comparative SA effect on k_w between sites we normalized our derived k_{660} values to the value of k_{660} derived in identical experiments in which the seawater samples were replaced by surfactant-free Milli-Q water (i.e. $R_{660} = k_{660\text{Sample}} / k_{660\text{Milli-Q}}$) (Schneider-Zapp et al., 2014).

Results and Discussion

Fig. 2 and Table 2 shows the spatial and temporal variability of SA, CDOM absorbance at 250–450 nm (CDOM₂₅₀₋₄₅₀), $E_2 : E_3$ and S_R . For all four parameters temporal variability generally exceeded spatial variability, both in the SML and in SSW. SA was generally higher in the SML than in SSW, as previously observed (e.g. Wurl et al., 2011). In both it was highest during June–July (SML; 0.25 - 0.38 mg l⁻¹ T-X-100, n = 8, SSW; 0.09 - 0.28 mg l⁻¹ T-X-100, n = 8) and lowest during October–February (SML; 0.08 - 0.27 mg l⁻¹ T-X-100, n = 10, SSW; 0.09 - 0.19

115 mg l⁻¹, n = 10). There is a clear relationship between SA in the SML and SSW ($r^2 = 0.81$ p = 0.001 n = 18) as



expected and SA enrichment factors (EF) for the SML relative to SSW were $\sim 1.0 - 1.9$, except for 2 samples collected in February 2013 for which SA was more enriched in SSW (EFs = 0.75 and 0.89, respectively). While in SSW there was an overall decrease in SA with increasing distance offshore, SA in the SML was more spatially and temporally variable (Fig. 2). Although two surveys (04/10/12; 10/06/13) clearly show an overall decrease in SA offshore the evidence is inconclusive as the remaining two transect shows either no clear overall trend (13/02/13) or are incomplete, (17/07/13).

S_R also showed high spatial and temporal variability (SML; 1.11 - 1.99, $n = 15$, SSW; 1.37 - 2.25, $n = 15$). It was generally higher in the SSW than the SML and it exhibited both increases and decreases with distance offshore. Unlike SA, this latter behaviour characterized both the SML and SSW (Fig. 2). In October 2012 S_R generally increased with distance offshore but in February and June 2013 it generally decreased offshore. $CDOM_{250-450}$ and $E_2 : E_3$ followed spatial trends that were more uniform overall, both in the SML and in SSW. $CDOM_{250-450}$ was generally higher in the SML than in SSW (EFs = 0.8 - 1.8), similar to the case for SA, whereas $E_2 : E_3$ was generally lower in the SML than in SSW (EFs = 0.7 - 1.1), similar to S_R (EFs = 0.6 - 1.2). While $CDOM_{250-450}$ decreased offshore by up to a factor ~ 4 (166 - 875) in both the SML and SSW, $E_2 : E_3$ showed an opposite tendency, progressively increasing seaward by up to a factor ~ 4 (2.3 - 8.43). In earlier work $E_2 : E_3$ was considered largely independent of total CDOM absorbance (Helms et al., 2008); however we observed relationships between $CDOM_{250-450}$ and $E_2 : E_3$ in both the SML ($r^2 = 0.45$ $p = 0.06$ $n = 15$) and in SSW ($r^2 = 0.69$ $p = 0.001$ $n = 15$). In contrast, we found no consistent relationship for either $CDOM_{250-450}$ or $E_2 : E_3$ with S_R . We tentatively propose that the divergence we specifically observed between $E_2 : E_3$ and S_R in February and June 2013 may be related to additional HMW CDOM “marine endmembers” during this period. However, establishing the cause of this divergence unequivocally will require additional surveys coupled with more advanced molecular characterization of DOM.

We similarly interpret the observed temporal variability in SA as a consequence of mixing between SA arising from at least two distinct marine and terrestrial endmembers. Likely candidates are terrestrially-derived SA from the nearby River Blyth and autochthonous SA from *in situ* biological activity. The relatively high SA and $CDOM_{250-450}$ at site 1 (0 km, directly at the mouth of the river), which is a persistent feature of the data, is consistent with this explanation if it is assumed that terrestrial endmember SA is higher than autochthonous SA. Furthermore, despite the covariance between $E_2 : E_3$ and $CDOM_{250-350}$, the overall decrease in $CDOM_{250-450}$ and increase $E_2 : E_3$ with distance offshore implies dilution of terrestrially derived CDOM with LMW marine CDOM. This is consistent with either HMW CDOM breakdown by photochemical or microbial processes (e.g. Helms et al., 2008; 2013) or an *in situ* supply of LMW CDOM to the most seaward sites. Either of these processes could explain the observed relationship between $E_2 : E_3$ and $CDOM_{250-450}$. As for total SA, these data reveal a clear compositional distinction between the SML and SSW. The generally higher SSW values of S_R and $E_2 : E_3$ noted earlier suggest that SML DOM is predominantly of HMW, as compared to predominantly LMW DOM in SSW. Although River Blyth discharge data [National River Flow Archive Centre for Ecology and Hydrology; <http://www.ceh.ac.uk/data/nrfa/>] show no clear relationship between river flow and either SA or $CDOM$ at site 1, our observations of SA and $CDOM_{250-450}$ are broadly consistent with the results of a study in Cape Cod coastal waters (Frew et al., 2004), although in that study the offshore gradients in SA were much stronger than those we



found off the NE UK coast. We also note that the River Blyth is rather small (mean annual discharge $\sim 2 \text{ m}^3 \text{ s}^{-1}$) and this is reflected in the very weak salinity gradients that we observed (range typically ± 0.6).

160 The values we derived for k_{660} using our gas exchange tank (6.82 to 22.06 cm hr^{-1}) are realistic in that they are within the reported natural k_{660} range of 5.81 to 70.17 cm hr^{-1} (Asher, 2009). Even so, it was not our intention to reproduce conditions leading to the generation of turbulence *in situ*, which is in any case unachievable in a laboratory setting due to the multiple and variable controls of both water- and air-side turbulence (Upstill-Goddard, 2006). It is also important to reiterate that our approach was specifically designed to produce comparative k_{660} estimates at controllable and reproducible turbulence levels and that as such, the mode of
165 turbulence generation (water-side: motor driven baffle) is of secondary importance. Generally we found increasing k_{660} with increasing water-side turbulence, as would be expected (Table 3). Even so, at the highest turbulence setting the data were comparatively noisy.

We found a strong correlation between R_{660} in our tank experiments and SA in the SML *in situ*. The strongest
170 linear relationships were observed at 0.6 Hz ($r^2 = 0.61$, $p = 0.001$, $n = 16$) and 0.7 Hz ($r^2 = 0.70$, $p = 0.001$, $n = 16$). At 0.75 Hz the linear relationship was notably weaker ($r^2 = 0.49$, $p = 0.02$, $n = 16$) and only when a non-linear relationship is considered does the correlation coefficient improve. Although this could imply a threshold level of turbulence beyond which the surfactant effect on k_{660} is rapidly attenuated *in situ*, we think it more likely indicates the limitations of the method at high baffle speeds due to the formation of bubbles and/or wave breaking and
175 aerosol generation. We observed a similar phenomenon with an earlier gas exchange tank design (Upstill-Goddard et al., 2003). More data is required to distinguish these scenarios and to robustly determine the relation between SA and R_{660} . On contrary, we found no significant relationships between R_{660} and either $\text{CDOM}_{250-450}$, S_R or E_2 : E_3 *in situ*.

180 Our derived R_{660} values (Fig. 3 and Table 3) correspond to k_{660} suppressions of 14 - 51 % for our samples ($R_{660} = 0.86 - 0.49$, $n = 48$) and highlight the effect of k_w suppression by natural surfactants in seawater compared to surfactant-free water. In our study we generally observed that k_w suppression was higher (i.e., lowest R_{660}) at near-shore sites ($< 5 \text{ km}$) than at off-shore sites ($> 5 \text{ km}$). This is most clearly shown for k_{660} derived for the lowest turbulence setting (0.6 Hz) in June 2013, for which R_{660} at the at the most near-shore site was ~ 10 % lower than
185 at the most offshore site. We also observed the largest seasonal variance in R_{660} at the most near-shore site; the change in k_w suppression ranged from 15 to 24 % (Fig. 3). Site 3 located 10 km offshore showed the highest variance in R_{660} at the highest baffle setting but was consistently observed to show a high variability in R_{660} between summer (June/July) and winter (October/February) regardless of changes in turbulence. The range of k_w suppressions we observed (15 - 24 %) is within the range of previous laboratory work that demonstrated 10 - 90
190 % surfactant suppression of O_2 exchange for oceanic and coastal waters (Frew, 1997; Goldman et al., 1988) and k_w reductions of 5 - 50 % for phytoplankton exudates (Frew et al., 1990). Similarly, laboratory and field experiments with artificial surfactants found 60 - 74 % k_w suppression (Bock et al., 1999; Frew, 1997; Salter et al., 2011). Even though we used SSW (1 metre) in the tank experiments this correlation does not surprise us given firstly that the SML rapidly re-establishes itself following water column disruption (Cunliffe et al., 2013) and



195 secondly that a SML has been shown to become rapidly established on sub-surface coastal waters pumped into mesocosm tanks (Cunliffe et al., 2009).

Given that our methodological approach was specifically designed to constrain the effect of surfactants in the SML on k_w and that this minimized the effects of other potential k_w controls, our observations of distinct changes in the quantity and composition of DOM in the SML and SSW prompt us to hypothesize that the observed spatio-temporal variation in R_{660} and its relationship with SA (Fig. 3) is a consequence of compositional differences in the surfactant fraction of the SML DOM pool. Such differences must incorporate components related to, for example, variations in productivity, anthropogenic surfactant sources, wind regime and hydrography (e.g. Chen et al., 2013; Frew et al., 2006; Gasparovic et al., 2007; Lechtenfeld et al., 2013).

205 Implications

Understanding the physical and biogeochemical controls of air–sea gas exchange is necessary for establishing biogeochemical models for predicting regional- and global-scale trace gas fluxes and feedbacks. Our results demonstrate the potential of our gas exchange tank concept in providing important information of this nature. In estimating ocean CO_2 uptake for example, the spatio-temporal variability of k_w is now a much larger uncertainty than the spatio-temporal variability of $p\text{CO}_2$ (Takahashi et al., 2009). For CO_2 and other climate-active gases that have strong sources and sinks in coastal waters (e.g. CH_4 , N_2O , halocarbons) it is equally important to quantify the degree of spatio-temporal variability in k_w so as to better constrain regional trace gas budgets (Prowe et al., 2009; Thomas et al., 2004; Thomas et al., 2007; Tsunogai et al., 1999). Clearly, this must involve resolving the influence on k_w exerted not only by changes in total surfactant amount in the SML but also by variability in the composition of the surfactant pool and in the composition of the overall DOM pool. We anticipate that further seasonal measurements of the type described in this paper, both at coastal and ocean basin scales, will move us some way towards an eventual full parameterization of the environmental controls of k_w , and in particular the evidently important roles played by spatial and temporal trends in both surfactant amount and composition.

Acknowledgements

220 This research was facilitated by grants from the Leverhulme Trust (RPG-303) and the UK Natural Environment Research Council (NE/I015299/1) to RCUG and from the German Research Foundation (DFG research fellowship) to KSZ. We also thank the crew of RV *Princess Royal* for field and logistical support, and Juliane Bischoff, Jon Barnes, and David Whitaker for technical and analytical assistance.

References

225 Asher, W. E.: The effects of experimental uncertainty in parameterizing air-sea gas exchange using tracer experiment data, *Atmos. Chem. Phys.*, 9, 131-139, 10.5194/acp-9-131-2009, 2009.
Bakker, D. E., Bange, H., Gruber, N., Johannessen, T., Upstill-Goddard, R., Borges, A., Delille, B., Löscher, C., Naqvi, S. W., Omar, A., and Santana-Casiano, J. M.: Air-Sea Interactions of Natural Long-Lived Greenhouse



- Gases (CO₂, N₂O, CH₄) in a Changing Climate, in: *Ocean-Atmosphere Interactions of Gases and Particles*, edited by: Liss, P. S., and Johnson, M. T., Springer Earth System Sciences, Springer Berlin Heidelberg, 113-169, 2014.
- 230 Bock, E. J., Hara, T., Frew, N. M., and McGillis, W. R.: Relationship between air-sea gas transfer and short wind waves, *Journal of Geophysical Research-Oceans*, 104, 25821-25831, 10.1029/1999jc900200, 1999.
- Brockmann, U. H., Huhnerfuss, H., Kattner, G., Broecker, H. C., and Hentschel, G.: Artificial surface-films in the sea area near Sylt, *Limnology and Oceanography*, 27, 1050-1058, 10.4319/lo.1982.27.6.1050, 1982.
- 235 Chen, Y., Yang, G. P., Wu, G. W., Gao, X. C., and Xia, Q. Y.: Concentration and characterization of dissolved organic matter in the surface microlayer and subsurface water of the Bohai Sea, China, *Continental Shelf Research*, 52, 97-107, 10.1016/j.csr.2012.11.007, 2013.
- Ćosović, B., and Vojvodić, V.: The Application of ac Polarography to the Determination of Surface-Active Substances in Sea-Water, *Limnology and Oceanography*, 27, 361-368, 1982.
- 240 Cunliffe, M., Harrison, E., Salter, M., Schaefer, H., Upstill-Goddard, R. C., and Murrell, J. C.: Comparison and validation of sampling strategies for the molecular microbial analysis of surface microlayers, *Aquatic Microbial Ecology*, 57, 69-77, 10.3354/ame01330, 2009.
- Cunliffe, M.: Physiological and Metabolic Effects of Carbon Monoxide Oxidation in the Model Marine Bacterioplankton *Ruegeria pomeroyi* DSS-3, *Appl. Environ. Microbiol.*, 79, 738-740, 10.1128/aem.02466-12, 245 2013.
- Cunliffe M, W. O., Engel A, Frka S, Landing W, Latif MT, Yang G-P, Zappa C, Upstill-Goddard R, Gasparovic B, Lindroos A, Leal M, Vagle S, Ekau W, Stolle C, Soloviev A, Lass K: Guide to best practices to study the ocean's surface, *Marine Biological Association of the United Kingdom*, 118, 2014.
- Frew, N., Nelson, R., and Johnson, C.: Sea slicks: variability in chemical composition and surface elasticity, in: 250 *Marine Surface Films*, edited by: Gade, M., Hühnerfuss, H., and Korenowski, G., Springer Berlin Heidelberg, 45-56, 2006.
- Frew, N.: *The sea surface and global change*, Cambridge University Press, Cambridge; New York, 1997.
- Frew, N. M., Goldman, J. C., Dennett, M. R., and Johnson, A. S.: Impact of phytoplankton-generated surfactants on air-sea gas-exchange, *Journal of Geophysical Research-Oceans*, 95, 3337-3352, 10.1029/JC095iC03p03337, 255 1990.
- Frew, N. M., Bock, E. J., Schimpf, U., Hara, T., Haussecker, H., Edson, J. B., McGillis, W. R., Nelson, R. K., McKenna, S. P., Uz, B. M., and Jahne, B.: Air-sea gas transfer: Its dependence on wind stress, small-scale roughness, and surface films, *Journal of Geophysical Research-Oceans*, 109, 10.1029/2003jc002131, 2004.
- Garrett, W. D.: Collection of slick-forming materials from the sea surface, *Limnology and Oceanography*, 10, 260 602-605, 10.4319/lo.1965.10.4.0602, 1965.
- Gašparović, B., Ćosović, B., and Vojvodić, V.: Contribution of organic acids to the pool of surface active substances in model and marine samples using o-nitrophenol as an electrochemical probe, *Org. Geochem.*, 29, 1025-1032, 10.1016/s0146-6380(98)00055-2, 1998.
- Gasparovic, B., Plavsic, M., Cosovic, B., and Saliot, A.: Organic matter characterization in the sea surface 265 microlayers in the subarctic Norwegian fjords region, *Marine Chemistry*, 105, 1-14, 10.1016/j.marchem.2006.12.010, 2007.



- Goldman, J. C., Dennett, M. R., and Frew, N. M.: Surfactant effects on air sea gas-exchange under turbulent conditions, *Deep-Sea Research Part a-Oceanographic Research Papers*, 35, 1953-1970, 10.1016/0198-0149(88)90119-7, 1988.
- 270 Helms, J. R., Stubbins, A., Ritchie, J. D., Minor, E. C., Kieber, D. J., and Mopper, K.: Absorption spectral slopes and slope ratios as indicators of molecular weight, source, and photobleaching of chromophoric dissolved organic matter, *Limnology and Oceanography*, 53, 955-969, 10.4319/lo.2008.53.3.0955, 2008.
- Helms, J. R., Stubbins, A., Perdue, E. M., Green, N. W., Chen, H., and Mopper, K.: Photochemical bleaching of oceanic dissolved organic matter and its effect on absorption spectral slope and fluorescence, *Marine Chemistry*, 275, 155, 81-91, 10.1016/j.marchem.2013.05.015, 2013.
- Hu, C. M., Muller-Karger, F. E., and Zepp, R. G.: Absorbance, absorption coefficient, and apparent quantum yield: A comment on common ambiguity in the use of these optical concepts, *Limnology and Oceanography*, 47, 1261-1267, 2002.
- Lechtenfeld, O. J., Koch, B. P., Gašparović, B., Frka, S., Witt, M., and Kattner, G.: The influence of salinity on the molecular and optical properties of surface microlayers in a karstic estuary, *Marine Chemistry*, 150, 25-38, 10.1016/j.marchem.2013.01.006, 2013.
- McKenna, S. P., and McGillis, W. R.: The role of free-surface turbulence and surfactants in air-water gas transfer, *International Journal of Heat and Mass Transfer*, 47, 539-553, 10.1016/j.ijheatmasstransfer.2003.06.001, 2004.
- Nightingale, P. D., Malin, G., Law, C. S., Watson, A. J., Liss, P. S., Liddicoat, M. I., Boutin, J., and Upstill-Goddard, R. C.: In situ evaluation of air-sea gas exchange parameterizations using novel conservative and volatile tracers, *Global Biogeochemical Cycles*, 14, 373-387, 10.1029/1999gb900091, 2000.
- 285 Petrović, M., Fernández-Alba, A. R., Borrull, F., Marce, R. M., Mazo, E. G., and Barceló, D.: Occurrence and distribution of nonionic surfactants, their degradation products, and linear alkylbenzene sulfonates in coastal waters and sediments in Spain, *Environmental Toxicology and Chemistry*, 21, 37-46, 10.1002/etc.5620210106, 2002.
- 290 Peuravuori, J., and Pihlaja, K.: Molecular size distribution and spectroscopic properties of aquatic humic substances, *Analytica Chimica Acta*, 337, 133-149, 10.1016/s0003-2670(96)00412-6, 1997.
- Prowe, A. E. F., Thomas, H., Patsch, J., Kuhn, W., Bozec, Y., Schiettecatte, L. S., Borges, A. V., and de Baar, H. J. W.: Mechanisms controlling the air-sea CO₂ flux in the North Sea, *Continental Shelf Research*, 29, 1801-1808, 10.1016/j.csr.2009.06.003, 2009.
- 295 Salter, M. E., Upstill-Goddard, R. C., Nightingale, P. D., Archer, S. D., Blomquist, B., Ho, D. T., Huebert, B., Schlosser, P., and Yang, M.: Impact of an artificial surfactant release on air-sea gas fluxes during Deep Ocean Gas Exchange Experiment II, *Journal of Geophysical Research-Oceans*, 116, 10.1029/2011jc007023, 2011.
- Schmidt, R. and Schneider B.: The effect of surface films on the air-sea gas exchange in the Baltic Sea, *Marine Chemistry*, 126:56-62, 10.1016/j.marchem.2011.03.007, 2011.
- 300 Schneider-Zapp, K., Salter, M. E., Mann, P. J., and Upstill-Goddard, R. C.: Technical Note: Comparison of storage strategies of sea surface microlayer samples, *Biogeosciences*, 10, 4927-4936, 10.5194/bg-10-4927-2013, 2013.
- Schneider-Zapp, K., Salter, M. E., and Upstill-Goddard, R. C.: An automated gas exchange tank for determining gas transfer velocities in natural seawater samples, *Ocean Sci.*, 10, 587-600, 10.5194/os-10-587-2014, 2014.
- 305 Takahashi, T., Sutherland, S. C., Wanninkhof, R., Sweeney, C., Feely, R. A., Chipman, D. W., Hales, B., Friederich, G., Chavez, F., Sabine, C., Watson, A., Bakker, D. C. E., Schuster, U., Metzl, N., Yoshikawa-Inoue,



- H., Ishii, M., Midorikawa, T., Nojiri, Y., Körtzinger, A., Steinhoff, T., Hoppema, M., Olafsson, J., Arnarson, T. S., Tilbrook, B., Johannessen, T., Olsen, A., Bellerby, R., Wong, C. S., Delille, B., Bates, N. R., and de Baar, H. J. W.: Climatological mean and decadal change in surface ocean pCO₂, and net sea-air CO₂ flux over the global oceans, *Deep-Sea Research Part II: Topical Studies in Oceanography*, 56, 554-577, 10.1175/1520-0442(2002)015
- 310 Tayler, J. R.: An introduction to error analysis: the study of uncertainties in physical measurements University Science Books, Sausalito, 1996.
- Thomas, H., Bozec, Y., Elkalay, K., and de Baar, H. J. W.: Enhanced open ocean storage of CO₂ from shelf sea pumping, *Science*, 304, 1005-1008, 10.1126/science.1095491, 2004.
- 315 Thomas, H., Prowe, A. E. F., van Heuven, S., Bozec, Y., de Baar, H. J. W., Schiettecatte, L. S., Suykens, K., Kone, M., Borges, A. V., Lima, I. D., and Doney, S. C.: Rapid decline of the CO₂ buffering capacity in the North Sea and implications for the North Atlantic Ocean, *Global Biogeochemical Cycles*, 21, 10.1029/2006gb002825, 2007.
- Tsunogai, S., Watanabe, S., and Sato, T.: Is there a “continental shelf pump” for the absorption of atmospheric
- 320 CO₂?, *Tellus B*, 51, 701-712, 10.1034/j.1600-0889.1999.t01-2-00010.x, 1999.
- Upstill-Goddard, R. C., Frost, T., Henry, G. R., Franklin, M., Murrell, J. C., and Owens, N. J. P.: Bacterioneuston control of air-water methane exchange determined with a laboratory gas exchange tank, *Global Biogeochemical Cycles*, 17, Artn 1108 10.1029/2003gb002043, 2003.
- Upstill-Goddard, R. C.: Air-sea gas exchange in the coastal zone, *Estuarine, Coastal and Shelf Science*, 70, 388-
- 325 404, 10.1016/j.ecss.2006.05.043, 2006.
- Wanninkhof, R.: Relationship between Wind-Speed and Gas-Exchange over the Ocean, *Journal of Geophysical Research-Oceans*, 97, 7373-7382, 10.1029/92jc00188, 1992.
- Wanninkhof, R., Hitchcock, G., Wiseman, W. J., Vargo, G., Ortner, P. B., Asher, W., Ho, D. T., Schlosser, P., Dickson, M.-L., Masserini, R., Fanning, K., and Zhang, J.-Z.: Gas exchange, dispersion, and biological
- 330 productivity on the West Florida Shelf: Results from a Lagrangian Tracer Study, *Geophysical Research Letters*, 24, 1767-1770, 10.1029/97gl01757, 1997.
- Wanninkhof, R., and McGillis, W. R.: A cubic relationship between air-sea CO₂ exchange and wind speed, *Geophysical Research Letters*, 26, 1889-1892, 10.1029/1999gl900363, 1999.
- Wurl, O., Miller, L., and Vagle, S.: Production and fate of transparent exopolymer particles in the ocean, *Journal of Geophysical Research-Oceans*, 116, 10.1029/2011jc007342, 2011.
- 335 Žutić, V., Čosović, B., Marčenko, E., Bihari, N., and Kršinić, F.: Surfactant Production by Marine-Phytoplankton, *Marine Chemistry*, 10, 505-520, 10.1016/0304-4203(81)90004-9, 1981.



Figure Captions

- 340 Figure 1: Location map of the Dove Time Series Sampling transect 2012-2013 off the coast of Blyth, North East England.
- Figure 2: Surfactant activity (normalized to Triton T-X-100), CDOM (250-450 nm), S_R and $E_2 : E_3$ ratio of the sea surface microlayer (SML; top panels) and sub-surface water (SSW; bottom panels) from a North Sea transect during 2012-2013.
- 345 Figure 3: Right panels are R_{660} for CH_4 in seawater samples collected along the Dove Time Series transect in the North Sea during 2012-2013. Left panels are scatterplots of the R_{660} ($R_{660} = k_{660\text{Sample}} / k_{660\text{Milli-Q}}$) and surfactant activity (SA) in the SML. The top two windows are for a tank baffle frequency of 0.6 Hz, the two middle windows are for a tank baffle frequency 0.7 Hz and bottom two windows are for a tank baffle frequency of 0.75 Hz.



350 **Tables**

Table 1: Sampling station number and location.

Dove Station Number	Sampling Locations (latitude, longitude)
1	55.11628, -1.45713
2	55.11642, -1.40918
3	55.11667, -1.33333
4	55.11665, -1.25675
5	55.11672, -1.18058



Table 2: Surfactant activity (normalized to Triton T-X-100), total CDOM absorbance (250–450 nm), S_R and $E_2 : E_3$ ratio of the sea surface microlayer (SML) and sub-surface water (SSW) from a North Sea transect during 2012–2013.

Date	Dove Station	Water	SA	CDOM _{250–450}	$S_{275–295}$	$S_{350–400}$	S_R	$E_2 : E_3$	Salinity
			mg l ⁻¹ T-X-100		nm ⁻¹	nm ⁻¹			
04/10/12	1	SML	0.27	874.8	0.013	0.010	1.32	3.580	
			±0.03	±37.6	±0.001	±0.001	±0.01	±0.250	
04/10/12	2	SML	0.22	429.0	0.016	0.008	1.99	4.291	
			±0.08	±156.7	±0.002	±0.004	±0.01	±1.026	
04/10/12	3	SML	0.17	240.4	0.021	0.014	1.54	6.832	
			±0.03	±6.8	±0.001	±0.001	±0.01	±0.208	
04/10/12	4	SML	0.15	250.6	0.021	0.013	1.62	6.584	
			±0.02	±12.8	±0.001	±0.001	±0.01	±0.177	
04/10/12	5	SML	0.14	261.1	0.020	0.012	1.73	6.009	
			±0.02	±33.3	±0.001	±0.001	±0.01	±0.385	
13/02/13	1	SML	0.11	637	0.010	0.005	1.91	2.459	
			±0.01	±158.5	±0.002	±0.003	±0.01	±0.561	
13/02/13	2	SML	0.08	339.1	0.014	0.008	1.74	3.847	
			±0.01	±12.8	±0.001	±0.001	±0.01	±0.062	
13/02/13	3	SML	0.13	452.1	0.013	0.009	1.51	3.556	
			±0.03	±12.2	±0.001	±0.001	±0.01	±0.132	
13/02/13	4	SML	0.10	326.0	0.016	0.009	1.71	4.179	
			±0.01	±23.8	±0.001	±0.001	±0.01	±0.205	
13/02/13	5	SML	0.11	322.6	0.016	0.011	1.47	4.236	
			±0.03	±14.3	±0.001	±0.001	±0.01	±0.109	
10/06/13	1	SML	0.30	379.0	0.020	0.011	1.85	5.849	
			±0.03	±10.8	±0.001	±0.001	±0.01	±0.124	
10/06/13	2	SML	0.29	409.8	0.019	0.011	1.74	5.640	
			±0.01	±41.9	±0.001	±0.001	±0.01	±0.206	
10/06/13	3	SML	0.30	328.5	0.020	0.012	1.71	6.188	
			±0.01	±11.7	±0.001	±0.001	±0.01	±0.086	
10/06/13	4	SML	0.28	400.5	0.016	0.015	1.11	5.162	
			±0.01	±10.5	±0.001	±0.001	±0.01	±0.055	
10/06/13	5	SML	0.25	326.9	0.018	0.014	1.29	5.832	
			±0.01	±13.2	±0.001	±0.001	±0.01	±0.067	
17/07/13	1	SML	0.38						
			±0.04						
17/07/13	2	SML	0.25						
			±0.05						
17/07/13	3	SML	0.28						
			±0.05						
17/07/13	4	SML							
17/07/13	5	SML							



Date	Dove Station	Water	SA	CDOM ₂₅₀₋₄₅₀	S ₂₇₅₋₂₉₅	S ₃₅₀₋₄₀₀	S _R	E ₂ : E ₃	Salinity
			mg l ⁻¹ T-X-100		nm ⁻¹	nm ⁻¹			
04/10/12	1	SSW	0.19 ±0.05	530.5 ±0.7	0.015 ±0.001	0.011 ±0.001	1.37 ±0.01	4.21 ±0.04	33.1
04/10/12	2	SSW	0.12 ±0.01	241.5 ±5.5	0.020 ±0.001	0.013 ±0.001	1.59 ±0.01	6.44 ±0.19	34.0
04/10/12	3	SSW	0.12 ±0.01	240.0 ±3.5	0.021 ±0.001	0.013 ±0.001	1.60 ±0.01	6.66 ±0.08	34.0
04/10/12	4	SSW	0.11 ±0.01	227.2 ±3.8	0.021 ±0.001	0.013 ±0.001	1.63 ±0.01	6.60 ±0.11	34.2
04/10/12	5	SSW	0.12 ±0.01	220.3 ±0.8	0.021 ±0.001	0.013 ±0.001	1.65 ±0.01	6.74 ±0.08	34.1
13/02/13	1	SSW	0.12 ±0.01	792.2 ±10.7	0.009 ±0.001	0.005 ±0.001	1.80 ±0.01	2.25 ±0.10	33.8
13/02/13	2	SSW	0.10 ±0.02	376.0 ±34.3	0.014 ±0.001	0.007 ±0.001	1.93 ±0.01	3.42 ±0.25	33.9
13/02/13	3	SSW	0.10 ±0.01	478.3 ±9.9	0.013 ±0.001	0.008 ±0.001	1.65 ±0.01	3.30 ±0.01	33.5
13/02/13	4	SSW	0.09 ±0.02	377.1 ±24.4	0.017 ±0.001	0.008 ±0.001	2.14 ±0.01	3.95 ±0.03	33.9
13/02/13	5	SSW	0.11 ±0.03	292.4 ±2.3	0.016 ±0.001	0.009 ±0.001	1.80 ±0.01	4.32 ±0.10	33.7
10/06/13	1	SSW	0.27 ±0.01	322.8 ±2.1	0.020 ±0.001	0.009 ±0.001	2.25 ±0.01	5.93 ±0.04	33.6
10/06/13	2	SSW	0.28 ±0.01	284.1 ±3.2	0.021 ±0.001	0.010 ±0.001	2.20 ±0.01	6.55 ±0.08	34.1
10/06/13	3	SSW	0.28 ±0.01	261.9 ±0.8	0.022 ±0.001	0.011 ±0.001	2.02 ±0.01	7.05 ±0.06	34.0
10/06/13	4	SSW	0.26 ±0.01	253.8 ±1.0	0.021 ±0.001	0.011 ±0.001	1.95 ±0.01	7.26 ±0.11	34.2
10/06/13	5	SSW	0.24 ±0.01	217.2 ±1.2	0.023 ±0.001	0.013 ±0.001	1.76 ±0.01	8.43 ±0.14	34.2
17/07/13	1	SSW	0.25 ±0.01						34.6
17/07/13	2	SSW	0.25 ±0.01						34.4
17/07/13	3	SSW	0.25 ±0.01						34.3
17/07/13	4	SSW							34.5
17/07/13	5	SSW							34.6

Table 3: k_{660} and R_{660} estimates from North East coast transect 2012-2013

Date	Dove Station	CH ₄ k_{660}			CH ₄ R_{660}		
		0.6 Hz	0.7 Hz	0.75 Hz	0.6 Hz	0.7 Hz	0.75 Hz
04/10/12	1	9.58 ±0.52	11.21 ±0.45	11.40 ±0.28	0.60 ±0.03	0.70 ±0.03	0.72 ±0.02
04/10/12	2	9.39 ±0.48	11.51 ±0.46	11.02 ±0.26	0.59 ±0.03	0.72 ±0.03	0.69 ±0.02
04/10/12	3	9.58 ±0.52	12.62 ±0.52	11.25 ±0.29	0.60 ±0.03	0.79 ±0.03	0.71 ±0.02
04/10/12	4	10.50 ±0.40	12.32 ±0.49	10.66 ±0.31	0.66 ±0.02	0.77 ±0.03	0.67 ±0.02
04/10/12	5	12.25 ±0.55	13.59 ±0.57	12.77 ±0.34	0.77 ±0.03	0.85 ±0.04	0.80 ±0.02
13/02/13	1	12.17 ±0.56	12.79 ±0.55	12.72 ±0.35	0.76 ±0.04	0.80 ±0.03	0.80 ±0.02
13/02/13	2						
13/02/13	3	12.68 ±0.66	13.67 ±0.56	11.16 ±0.42	0.80 ±0.04	0.86 ±0.04	0.70 ±0.03
13/02/13	4	10.97 ±0.46	13.21 ±0.53	12.55 ±0.34	0.69 ±0.03	0.83 ±0.03	0.79 ±0.02
13/02/13	5	13.04 ±0.51	13.6 ±0.54	13.11 ±0.37	0.82 ±0.03	0.85 ±0.03	0.82 ±0.02
10/06/13	1	8.17 ±0.37	9.05 ±0.40	8.70 ±0.44	0.51 ±0.02	0.57 ±0.02	0.55 ±0.03
10/06/13	2	7.77 ±0.33	8.93 ±0.37	8.65 ±0.25	0.49 ±0.02	0.56 ±0.02	0.54 ±0.02
10/06/13	3	8.02 ±0.33	10.46 ±0.43	11.54 ±0.42	0.50 ±0.02	0.66 ±0.03	0.72 ±0.03
10/06/13	4						
10/06/13	5	9.51 ±0.38	10.52 ±0.44	9.83 ±0.26	0.60 ±0.02	0.66 ±0.03	0.62 ±0.02
17/07/13	1	9.71 ±0.41	10.92 ±0.47	10.13 ±0.36	0.61 ±0.03	0.69 ±0.03	0.64 ±0.02
17/07/13	2	10.29 ±0.54	9.94 ±0.47	9.50 ±0.24	0.65 ±0.03	0.62 ±0.03	0.60 ±0.02
17/07/13	3	10.02 ±0.62	11.15 ±0.48	7.91 ±3.90	0.63 ±0.04	0.70 ±0.03	0.50 ±0.02
17/07/13	4						
17/07/13	5						



365 Figure 1



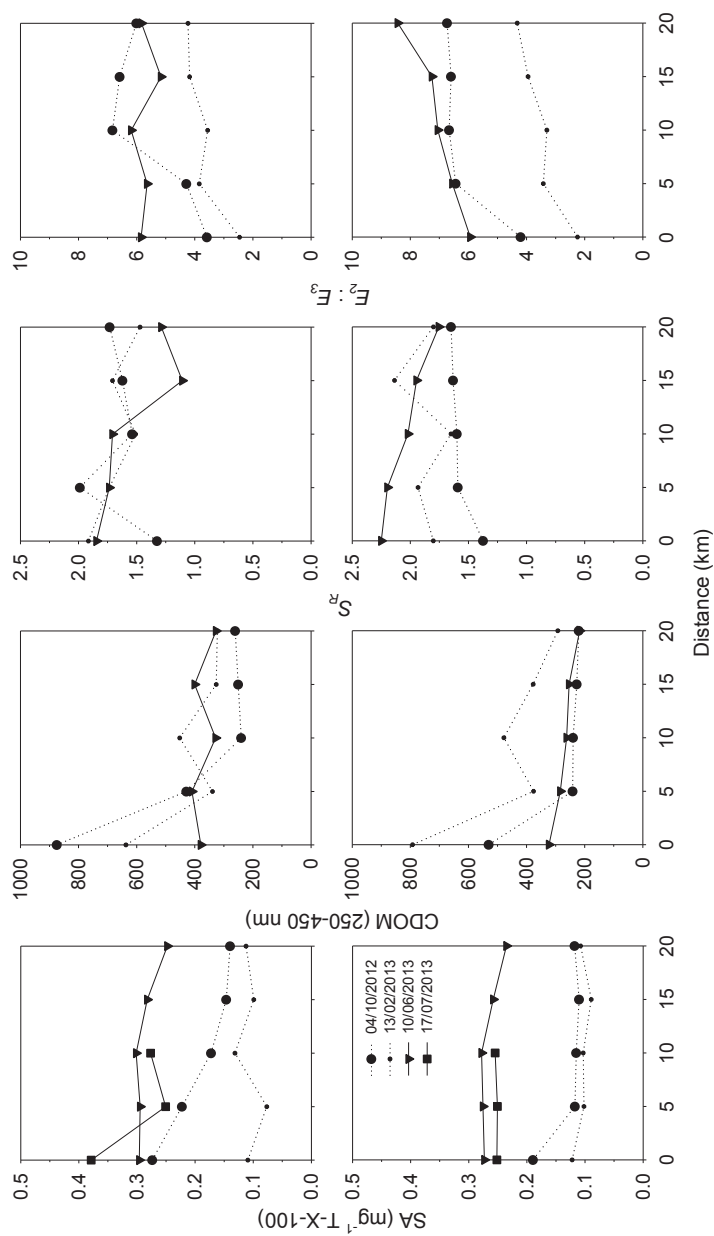


Figure 2



Figure 3

